FEMS Microbiology Ecology, 96, 2019, fiz187

doi: 10.1093/femsec/fiz187
Advance Access Publication Date: 26 November 2019
Research Article

RESEARCH ARTICLE

Antibiotic-induced gut metabolome and microbiome alterations increase the susceptibility to *Candida albicans* colonization in the gastrointestinal tract

Daniel Gutierrez[1], Anthony Weinstock[2], Vijay C. Antharam[3], Haiwei Gu[4,†], Paniz Jasbi[4], Xiaojian Shi[4], Blake Dirks[5], Rosa Krajmalnik-Brown[5,6,7], Juan Maldonado[7], Jack Guinan[1] and Shankar Thangamani[8,*,‡]

[1]College of Veterinary Medicine, Midwestern University, 19555 N. 59th Ave. Glendale, AZ 85308, USA, [2]Arizona College of Osteopathic Medicine, Midwestern University, 19555 N. 59th Ave. Glendale, AZ 85308, USA, [3]Department of Chemistry, School of Science and Human Development, Methodist University, 5400 Ramsey St, Fayetteville, NC 28311, USA, [4]Arizona Metabolomics Laboratory, College of Health Solutions, Arizona State University, Phoenix, AZ 85259, USA, [5]Biodesign Swette Center for Environmental Biotechnology, Arizona State University, Tempe, AZ 85280, USA, [6]School of Sustainable Engineering and the Built Environment, Arizona State University, Tempe, AZ 85287, USA, [7]Biodesign Center for Fundamental and Applied Microbiomics, Biodesign Institute, Arizona State University, Tempe, AZ 85287, USA and [8]Department of Pathology and Population Medicine, College of Veterinary Medicine, Midwestern University, 19555 N. 59th Ave. Glendale, AZ 85308, USA

*Corresponding author: Department of Pathology and Population Medicine, College of Veterinary Medicine, Midwestern University, 19555 N. 59th Ave. Glendale, AZ 85308, USA. Tel: 623-537-6378; E-mail: sthang@midwestern.edu

One sentence summary: Gut metabolites and microbiome regulate the gastrointestinal colonization of *C. albicans*.

Editor: Tong Zhang
†Haiwei Gu, http://orcid.org/0000-0002-7598-5022
‡Shankar Thangamani, http://orcid.org/0000-0002-0031-2392

ABSTRACT

Antibiotic-induced alterations in the gut ecosystem increases the susceptibility to *Candida albicans*, yet the mechanisms involved remains poorly understood. Here we show that mice treated with the broad-spectrum antibiotic cefoperazone promoted the growth, morphogenesis and gastrointestinal (GI) colonization of *C. albicans*. Using metabolomics, we revealed that the cecal metabolic environment of the mice treated with cefoperazone showed a significant alteration in intestinal metabolites. Levels of carbohydrates, sugar alcohols and primary bile acids increased, whereas carboxylic acids and secondary bile acids decreased in antibiotic treated mice susceptible to *C. albicans*. Furthermore, using *in-vitro* assays, we

Received: 6 September 2019; **Accepted:** 25 November 2019

confirmed that carbohydrates, sugar alcohols and primary bile acids promote, whereas carboxylic acids and secondary bile acids inhibit the growth and morphogenesis of *C. albicans*. In addition, in this study we report changes in the levels of gut metabolites correlated with shifts in the gut microbiota. Taken together, our *in-vivo* and *in-vitro* results indicate that cefoperazone-induced metabolome and microbiome alterations favor the growth and morphogenesis of *C. albicans*, and potentially play an important role in the GI colonization of *C. albicans*.

Keywords: *Candida albicans*; metabolome; microbiome; growth; hyphal formation and gastrointestinal colonization

INTRODUCTION

Candida albicans, an opportunistic eukaryotic pathogen present in healthy gastrointestinal (GI) tracts, is harmless to the immunocompetent human host and co-exists harmlessly with resident microbiota (Fan *et al.* 2015; Neville, d'Enfert and Bougnoux 2015). *Candida albicans* colonization is normally asymptomatic and yeast cells often exist as avirulent entities in the gut ecosystem (Fan *et al.* 2015; Neville, d'Enfert and Bougnoux 2015). Emerging evidences indicate that *C. albicans* found in the gut have been increasingly found to contribute and play an active role in health and diseases by modulating the gut–brain axis and elevating *Clostridium difficile* infections. These examples demonstrate the newly appreciated role of the mycobiome in human health (Gerard *et al.* 2015; Kantarcioglu, Kiraz and Aydin 2016; Chu *et al.* 2018; Enaud *et al.* 2018; Stamatiades *et al.* 2018; Tso *et al.* 2018; Zuo *et al.* 2018). Therefore, elucidating the GI colonization of *C. albicans* will have broad implications for our understanding of the gut mycobiome, which is an underappreciated aspect of microbiome research.

Although the majority of *C. albicans*–host interactions are asymptomatic, administration of broad-spectrum antibiotics increases the risk of *C. albicans* infections by increasing the frequency and magnitude of GI colonization by *C. albicans*; furthermore, the source of systemic infection is often confirmed to be the GI tract (Kennedy *et al.* 1987; Meijer-Severs and Joshi 1989; Samonis *et al.* 1993; Cole, Halawa and Anaissie 1996; Krause *et al.* 2001; Nucci and Anaissie 2001; Krause *et al.* 2003; Sahni *et al.* 2005; Miranda *et al.* 2009; Nerandzic *et al.* 2012; Guastalegname *et al.* 2013; Delaloye and Calandra 2014; Raponi *et al.* 2014; Zuo *et al.* 2018). The transition from yeast to hyphal cell morphology is central to *C. albicans* pathogenesis. Oval-shaped yeast cells begin to elongate and branch, creating a filamentous network that evolve to form hyphae. The ability of *C. albicans* to attach and disseminate from the GI tract is associated with its capacity to undergo a morphological transition from yeast to hyphae, which allows the organism to attach, invade and perpetuate disease (Lo *et al.* 1997; Gale *et al.* 1998; Bendel *et al.* 1999; Toenjes *et al.* 2005; Carlisle *et al.* 2009; Fazly *et al.* 2013; Pande, Chen and Noble 2013; Bar-Yosef *et al.* 2017; Mendelsohn *et al.* 2017; Vila *et al.* 2017). The mammalian GI tract is loaded with numerous signals that regulate *C. albicans* growth and morphogenesis, and therefore understanding of the microbiota and metabolite signatures that control this transition would provide insight into the balance between commensalism and invasive infection.

As many of the inter-species interactions in the gut are mediated by metabolites produced by the gut microbiota, recent findings indicate that metabolites secreted, modulated or degraded by the microbiome play a critical role in shaping susceptibility of the gut community to invading pathogens (Theriot *et al.* 2014; Buffie *et al.* 2015; Theriot, Bowman and Young 2016; Suez and Elinav 2017; Kohli *et al.* 2018; Seekatz *et al.* 2018). However, the role of gut metabolome in the GI colonization and pathogenesis of *C. albicans* is poorly understood. In mice and humans, antibiotic treatment not only alters the gut microbiota but ultimately changes the composition of the gut metabolites (Young and Schmidt 2004; Dethlefsen and Relman 2011; Theriot *et al.* 2014; Fan *et al.* 2015; Theriot, Bowman and Young 2016). Therefore, to better understand the complex interaction between *C. albicans*, the metabolome and the microbiome, we used a combination of mass spectrometry, 16S ribosomal RNA amplicon gene sequencing and *in-vitro* studies to define the functional changes in the gut that accompany the susceptibility to this fungal pathogen.

The results from this study along with our previous findings (Guinan and Thangamani 2018; Guinan, Villa and Thangamani 2018; Thangamani *et al.* 2018) indicate that alterations in the levels of gut metabolites as a result of antibiotic treatment correlate to increased growth and hyphae formation of *C. albicans* inhabiting the GI tract. The cecal contents of antibiotic-treated mice susceptible to *C. albicans* GI infection had significantly increased levels of carbohydrates and primary bile acids, and decreased levels of secondary bile acids and carboxylic acids. Furthermore, our results indicate that carbohydrates and primary bile acids promotes growth, whereas secondary bile acids and carboxylic acids inhibit *C. albicans* growth and morphogenesis *in vitro*. Taken together, this study indicates that altered levels of cecal metabolites in antibiotic-treated mice may remove an essential barrier to *C. albicans* overgrowth in the GI tracts of colonized animals, and may play a critical role in the GI colonization of this fungal pathogen.

MATERIALS AND METHODS

Mice studies

The *C. albicans* SC5314 strain used in this study was kindly provided by Dr. Andrew Koh (University of Texas Southwestern Medical Center) (Fan *et al.* 2015). Male and female C57BL/6 J mice (five to six mice per group) were supplemented with sterile water with or without cefoperazone (0.5 mg/mL) (Theriot *et al.* 2011). After 7 days of antibiotic treatment, groups of non-treated or cefoperazone treated mice were infected with *C. albicans* SC5314 via oral gavage at a dose of approximately 4×10^8 CFU per mice as described before (Guinan and Thangamani 2018). After 10 days of infection, fecal samples were collected from individual mice to determine the fungal load as described before (Guinan and Thangamani 2018). Briefly, 100 μL of homogenized fecal samples were serially diluted in PBS and plated on to YPD agar containing kanamycin, streptomycin and ampicillin to determine the fungal CFU count in fecal content. Mice were euthanized and the cecal contents were collected for metabolomics, microbiome analysis and *ex-vivo* assays.

Ex-vivo hyphae assays

Gut contents from non-treated and antibiotic treated C57BL/6 J mice were obtained. A totaol of 70–100 mg of each sample was added into 70–100 μL of PBS and vortexed vigorously for 30 seconds. The samples were then centrifuged at 1000 rpm for 2

minutes, and the supernatant was collected into a new 1.5 mL microcentrifuge tube. For the hyphae assay, two medium sized *C. albicans* SC5314 colonies were inoculated into 1 mL of 1X PBS and vortexed. 10 μL of PBS containing *C. albicans* SC5314 was added to 70 μL of each sample. Samples were then incubated at 37°C for 3 hours and centrifuged at 1000 rpm for 2 minutes and fixed with 2% paraformaldehyde. *Candida albicans* was stained using primary and secondary antibodies at a dilution of 1:100 and 1:500, respectively, as described before (Guinan and Thangamani 2018). After staining, fungal cells were gently resuspended in 100 μL of PBS and plated onto a non-treated sterile 96-well plate. Cells were then imaged (40X) using a Keyence BZ-X700 microscope and analyzed with Keyence Analyzer software.

Metabolomics

(i) *Aqueous Metabolites:* Frozen cecal samples were thawed, and the initial step for protein precipitation and metabolite extraction was performed by adding 500 μL MeOH and 50 μL internal standard solution (containing 1810.5 μM $^{13}C_3$-lactate and 142 μM $^{13}C_5$-glutamic acid). The mixture was then homogenized and vortexed for 10 seconds and stored at –20°C for 30 minutes, followed by centrifugation at 14 000 RPM for 10 minutes at 4°C. The supernatants collected were dried using a CentriVap Concentrator (Labconco, Fort Scott, KS). The dried samples were reconstituted in 40% PBS/60% ACN prior to LC-MS analysis. The targeted LC-MS/MS metabolomics was performed on an Agilent 1290 UPLC-6490 QQQ-MS system (Santa Clara, CA) as described before (Zhu *et al.* 2014; Carroll *et al.* 2015; Gu *et al.* 2015; Gu *et al.* 2016; Buas *et al.* 2017; Li *et al.* 2018a; Jasbi *et al.* 2019; Shi *et al.* 2019). Briefly, chromatographic separations were performed in hydrophilic interaction chromatography (HILIC) mode on a Waters XBridge BEH Amide column (150 × 2.1 mm, 2.5 μm particle size, Waters Corporation, Milford, MA). The flow rate was 0.3 mL/minute, auto-sampler temperature was kept at 4°C, and the column compartment was set to 40°C. The mobile phase was composed of Solvents A (10 mM ammonium acetate, 10 mM ammonium hydroxide in 95% H_2O/5% ACN) and B (10 mM NH_4OAc, 10 mM NH_4OH in 95% ACN/5% H_2O). After an initial 1-minute isocratic elution of 90% B, the percentage of Solvent B decreased to 40% at t = 11 minutes. The composition of Solvent B was maintained at 40% for 4 minutes (t = 15 minnutes), after which the percentage of B gradually went back to 90%, to prepare for the next injection. Mass spectroscopy was performed with an electrospray ionization (ESI) source. Targeted data acquisition was performed in multiple-reaction-monitoring (MRM) mode. We monitored 118 and 160 MRM transitions in negative and positive mode, respectively (278 transitions in total). The whole LC-MS system was controlled by Agilent MassHunter Workstation software (Santa Clara, CA).

(ii) *Bile Acid Analysis:* Bile acids were extracted from cecal contents using methods reported elsewhere (Zhang and Klaassen 2010; Ginos *et al.* 2018; Li *et al.* 2018b). Briefly, 60 mg frozen pellets of flushed intestinal content were homogenized with a 10 μL solution of five internal standards (CA-D_4, LCA-D_4, DCA-D_4, GCA-D_4 and GCDCA-D_4, 10 μM each) and methanol (500 μL), and then vortexed for 10 seconds. Samples were then stored at −20°C for 20 minutes for bile acid extraction, followed by sonication in an ice bath for 10 minutes, and centrifugation at 14 000 RPM for 15 minutes at 4°C. Supernatants (500 μL) were vacuum dried and then reconstituted in MeOH/H_2O (1:1, v/ v) to 100 μL. Each prepared sample (2 μL) was injected into the LC-MS system (Agilent 1290 UPLC-6490 QQQ-MS) for analysis using negative ionization mode. The mobile phase was composed of two solvents: 5 mM NH_4OAc in H_2O with 0.1% AcOH (A) and ACN with 0.1% AcOH (B). After 1 minute of isocratic elution of 75% solvent A, it decreased to 5% at t = 15 minutes. Composition was then maintained at 5% for 10 minutes, followed by an increase to 75% at t = 25 minutes. The total experimental time for each injection was 40 minutes. Bile acid identities were validated by spiking mixtures of standard compounds.

(iii) *Data Analysis:* Univariate testing was performed using SPSS 22.0 (SPSS Inc., Chicago, IL). Box plots of pertinent metabolites in addition to multivariate statistical analyses were performed using R. The data were $\log_{10}$-transformed prior to model construction. Heatmaps for detected metabolites were constructed and visualized using MetaboAnalyst software (Chong *et al.* 2018).

Screening gut metabolites against *C. albicans* growth

Freshly streaked colonies of *C. albicans* SC5314 were added to PBS to match 0.5 McFarland Standard turbidity and subsequently diluted 500-fold into YNB or RPMI media and seeded in 96-well microplates. *Candida albicans* was grown in the presence or absence of indicated gut metabolites and incubated at 30°C for 24 hours. After incubation, growth was measured using a spectrophotometer at $OD600_{nm}$ (BioTek Cytation 3). Carbohydrates and sugar alcohols were screened using YNB media with 0.05% ammonium sulfate; carboxylic acids that were dissolved using water or ethanol were screened using YNB media containing 0.05% ammonium sulfate and 0.2% D-glucose. Carboxylic acids dissolved in DMSO and bile acids were screened using RPMI media. Compounds were purchased from the commercial vendors and solvents used in this study were described in the supplementary materials.

Screening gut metabolites against *C. albicans* hyphae formation

The effect of gut metabolites on *C. albicans* hyphae was tested as described below. Three colonies of *C. albicans* SC5314 were added to 15-mL of RPMI + 30% FBS or YNB media. Media (500 μL) containing fungal cells were aliquoted to 1.5-mL tubes in the presence or absence of indicated gut metabolites and incubated at 37°C for 3–5 hours. After incubation, 1.5-mL tubes were vortexed vigorously and 5 to 20 μL were added to 96-well microplates containing 50 μL PBS. After *C. albicans* cells settled to the bottom of the wells, fungal cells were imaged using a Keyence BZ-X700 microscope at 40X magnification as described above in the *ex-vivo* assay. Carbohydrates were screened using YNB media with 0.05% ammonium sulfate. Carboxylic acids and inhibitory bile acids were screened in RPMI+ 30% FBS. Furthermore, primary bile acids were tested using YNB media containing 0.2% D-glucose.

Microbiome library preparation and sequencing

Bacterial community analysis was performed via next generation sequencing in MiSeq Illumina platform. Amplicon sequencing of the V4 region of the 16S rRNA gene was performed with the barcoded primer set 515f/806r designed by Caporaso *et al.* (2011) and following the protocol by the Earth Microbiome

Project (EMP) (http://www.earthmicrobiome.org/emp-standard-protocols/) for library preparation. PCR amplifications for each sample were done in triplicate, then pooled and quantified using Quant-iT™ PicoGreen® dsDNA Assay Kit (Invitrogen). A no template control sample is always included during the library preparation as a control for extraneous nucleic acid contamination. A total of 240 ng of DNA per sample were pooled and then cleaned using QIA quick PCR purification kit (QIAGEN). The pool was quantified by Illumina library Quantification Kit ABI Prism® (Kapa Biosystems). Then, the DNA pool was diluted to a final concentration of 4 nM then denatured and diluted to a final concentration of 4 pM with a 15% of PhiX. Finally, the DNA library was loaded in the MiSeq Illumina and run using the version 2 module, 2 × 250 paired-end, following the directions of the manufacturer.

Microbiome analysis

Microbiome sequences were analyzed using Qiime2 (2018.11.) Sequences were demultiplexed and filtered for quality using DADA2. Sequences were aligned using mafft and a phylogenetic tree was constructed from the aligned sequences by fasttree. Alpha diversity metrics (Observed OTUS, Evenness, Shannon's, and Faith's PD) and beta diversity metrics (weighted and unweighted unifrac distances, Bray–Curtis distance and Jaccard distance) were calculated with a sampling depth of 11 000. Taxonomic analysis was performed using a classifier trained with Greengenes 13_8 99% OTUs. Taxonomic bar plots were created using R (R Core Team) packages *Reshape* and ggplot2 (Caporaso *et al.* 2010). Relative abundances for OTUs were calculated in R using the *gplots* package. OTUs with less than 1% abundance across all samples were grouped together and categorized as 'Other'. Faith's Phylogenetic Diversity (Faith PD) was calculated with the Qiime2 pipeline. Kruskal–Wallis pairwise comparison was used to determine statistical significance (P value ≤ 0.05).

Microbiome and metabolome correlation analysis

A matrix of with metabolites (either from the carbohydrate or carboxylic acid compound class) were Spearman correlated to a matrix of phylum OTUs from the same group using the *Hmisc* package in Rstudio version 1.1447. The resulting correlation matrix was combined for Group A, Group B, Group C and Group D for heatmap visualization. The *RcolorBrewer* package alongside *gplots* were used for making heatmaps in a R studio environment.

PICRUSt analysis

Functional identification of 16S rRNA gene content as determined by PICRUSt was utilized for discriminatory analysis and biomarker assessment via LEfSe, a tool that determines candidate markers from multivariate data sets using a ranked-sum Kruskal–Wallis statistical test followed by linear discriminant analysis to determine the effect size for each putative marker (Segata *et al.* 2011; Langille *et al.* 2013; Berlanga, Palau and Guerrero 2018). Output from PICRUSt were inputted into the LEfSe pipeline to determine LDA (Linear discriminant analysis) scores for predicted functional identifications. From this, the four groups in this study were classified according to the most predicted prominent features. Based on a criteria of LDA score >3.00 and a statistical significance level of $P < 0.05$, the top features from each Group housed under metabolic compartments: amino acid metabolism, carbohydrate metabolism, cell wall metabolism, nucleotide metabolism, fatty acid metabolism and lipid metabolism. Other gene products implicated as differential but did not comport with the five groupings were classified as 'Other'. Due to the skewed dispersion of the predicted 16S rRNA gene counts, the PICRUSt was normalized to unity prior to visualization of the results via heatmap. After normalization of OTU counts from 0 to 1, the resulting matrix was plotted for all 4 groups using the heatmap.2 function in base R Studio version 1.1447.

Ethics statement

All animal protocols were approved by Midwestern University Institutional Animal Care and Use Committee (IACUC) as described before (Guinan and Thangamani 2018). The Institutional Animal Care and Use Committee at Midwestern University approved this study under MWU IACUC Protocol #2894. The MWU animal care policies follow the Public Health Service (PHS) Policy on Humane Care and Use of Laboratory Animals and the policies laid out in the Animal Welfare Act (AWA).

Statistical analysis

The Student t-test was utilized for statistical analyses using GraphPad Prism 6.0 (GraphPad Software, La Jolla, CA) with P values of ($^{*} \leq 0.05$, $^{**} \leq 0.01$) being considered significant.

RESULTS

Cefoperazone (cef)-treated mice promote the growth and morphogenesis of *C. albicans*

Given the previous reports that antibiotic treatment promotes the colonization of *C. albicans* in the murine GI tract (Wiesner *et al.* 2001; Fan *et al.* 2015; Schulte *et al.* 2015), we hypothesized that antibiotic induced changes in the gut metabolic environment favor GI colonization by *C. albicans*. To define the role of gut metabolites in the GI colonization of *C. albicans*, wild-type adult mice were given sterile water containing with or without the broad-spectrum antibiotic cefoperazone (Fig. 1A). One group of mice from the non-treated and cef-treated groups were infected with *C. albicans*. Following treatments and infection with *C. albicans*, mice in each group were split into two sets. Gut contents from one set were harvested for metabolome and microbiome analysis, while mice in the other set were euthanized to determine the fungal load in the feces to evaluate susceptibility to *C. albicans* (Fig. 1A).

As expected, cef-treated mice had an almost 4-log10 increase in fungal load in the feces compared to non-treated infected mice (Fig. 1B). Since hyphal morphogenesis has been established as a key virulence factor, we studied the effect of antibiotic treatment on *C. albicans* morphogenesis. *Candida albicans* colonize along the entire GI tract including the stomach, small intestine, cecum and large intestine (Bohm *et al.* 2017; Witchley *et al.* 2019). Therefore, we investigated the effect of antibiotic treatment on *C. albicans* hyphae morphogenesis in gut contents from different segments of the GI tract. Interestingly, our results indicate that *C. albicans* grown *ex vivo* from the stomach, small intestines and large intestines of non-treated and cef-treated mice mainly existed as the yeast form (Fig. 1C). However, *C. albicans* grown *ex vivo* in the cecal content from cef-treated, but not from control mice readily undergo morphogenesis and exist as a mixture of yeast and hyphae forms (Fig. 1C).

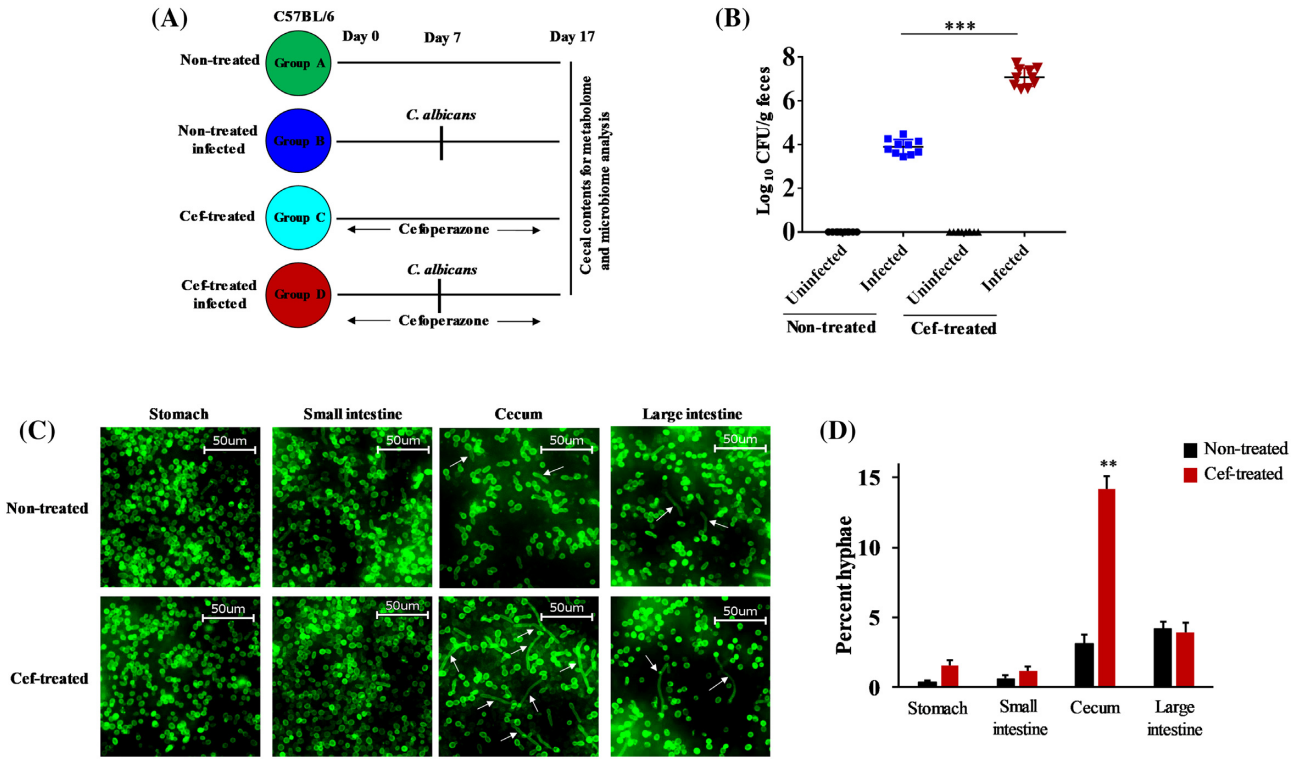

Figure 1. **(A)** Schematic diagram of the experimental design. **(B)** Fungal load in the feces of non-treated and cef-treated mice infected with or without *C. albicans*. *Candida albicans* SC5314 load in fecal contents at day 17 after infection in mice at day 7 receiving sterile water or cefoperazone-containing water. **(C)** Gut contents from non-treated and antibiotic (cef) treated adult mice were obtained and inoculated with *C. albicans* SC5314 *ex vivo* at 37°C for 3 hours and stained with *C. albicans* antibody. Cells were imaged at 40X using Keyence BZ-X700 microscope. Representative images are shown here. **(D)** Percent hyphae in gut contents from non-treated and cef-treated mice inoculated with *C. albicans ex vivo* were determined. Atleast 5 images were counted per group (n = 3). Data represented as means ± SEM. Statistical significance was evaluated using students t-test and *P* values (* ≤ 0.05, ** ≤ 0.01) were considered as significant.

The % of hyphae in the cecal content from cef-treated mice is significantly higher than non-treated mice. More than 10% of fungal cells grown *ex vivo* in cecal content from cef-treated mice undergone hyphal morphogenesis (Fig. 1D). These results suggest that cefoperazone-induced alterations in the cecum may potentially favor hyphal morphogenesis in *C. albicans*. In addition, fungal load (Fig. 1B) in feces have been shown to correlate to CFU counts in gut contents, including cecum (Guinan and Thangamani 2018). Taken together, these results indicate that cefoperazone treatment promotes the growth and morphogenesis of *C. albicans*, and potentially creates an environment favoring the GI colonization of pathogen.

Cefoperazone treatment alters the composition of cecal metabolome

To examine the composition of the cecal metabolome in the non-treated and cef-treated groups, cecal contents were analyzed using mass spectrometry to identify the metabolites belonging to the (i) Kyoto Encyclopedia of Genes and Genomes metabolic pathways (KEGG), which includes amino acids, carbohydrates, lipids, peptides, xenobiotics; and (ii) bile acids. Metabolites that were significantly different between non-treated and cef-treated groups are shown in heat map form (Fig. 2A and B and Figure S1–2, Supporting Information). The cecal metabolome of the cef-treated mice was associated with relative increases in carbohydrates and sugar alcohols compared to non-treated groups (Fig. 2A; Figure S1–2, S3 Data, Supporting Information). Treatment with cefoperazone increased the relative levels of adonitol, l-arabinose, dulcitol, galactinol, d-mannitol, lactose, trehalose and xylitol. The only carbohydrates to show a significant decrease were glucose and mannose. Furthermore, we examined if infection with *C. albicans* has any effect on these metabolites. Results indicate that *C. albicans* infection showed a considerable increase in xylose in both non-treated and cef-treated groups (Fig. 2A and Figure S2, Supporting Information).

While most carbohydrates and sugar alcohols significantly increased after cefoperazone treatment, the majority of other metabolites including amino acids, vitamins and carboxylic acids were significantly decreased in the cef-treated groups (Fig. 2A; Figure S2 and S3 Data, Supporting Information). The majority of the carboxylic acids examined were significantly lower in antibiotic treated mice compared to control groups. Phthalic, non-adecconic, azelaic, salicylic, leucic, p-tolyacetic, mandelic, glutamic, valeric, sebacic, pyroglutamic, pipercolinic, methylmalonic, urocanic, picolinic, pentadecanoic, ferulic and fumaric acid were consistent with this trend. The other carboxylic acids including citraconic acid, indoleacetic acid, malonic acid, suberic acid, shikimic acid, maleic acid, palmitic acid, glutaconic acid and hexanoic acid were considerably increased with antibiotic treatment. Infection with *C. albicans* in control adult mice had little effect on the majority of the gut metabolites except the levels of maleic acid, which showed an appreciable increase. However, we found that ketoleucine, citroconic acid, ferulic acid levels were decreased, whereas 2-deoxycytidine, cytosine, xanthosine, guanosine, guanine, inosine, uridine, fumaric acid, fumarate, citrulline, 2-deoxyguanosine, nicotinamide levels were higher in antibiotic

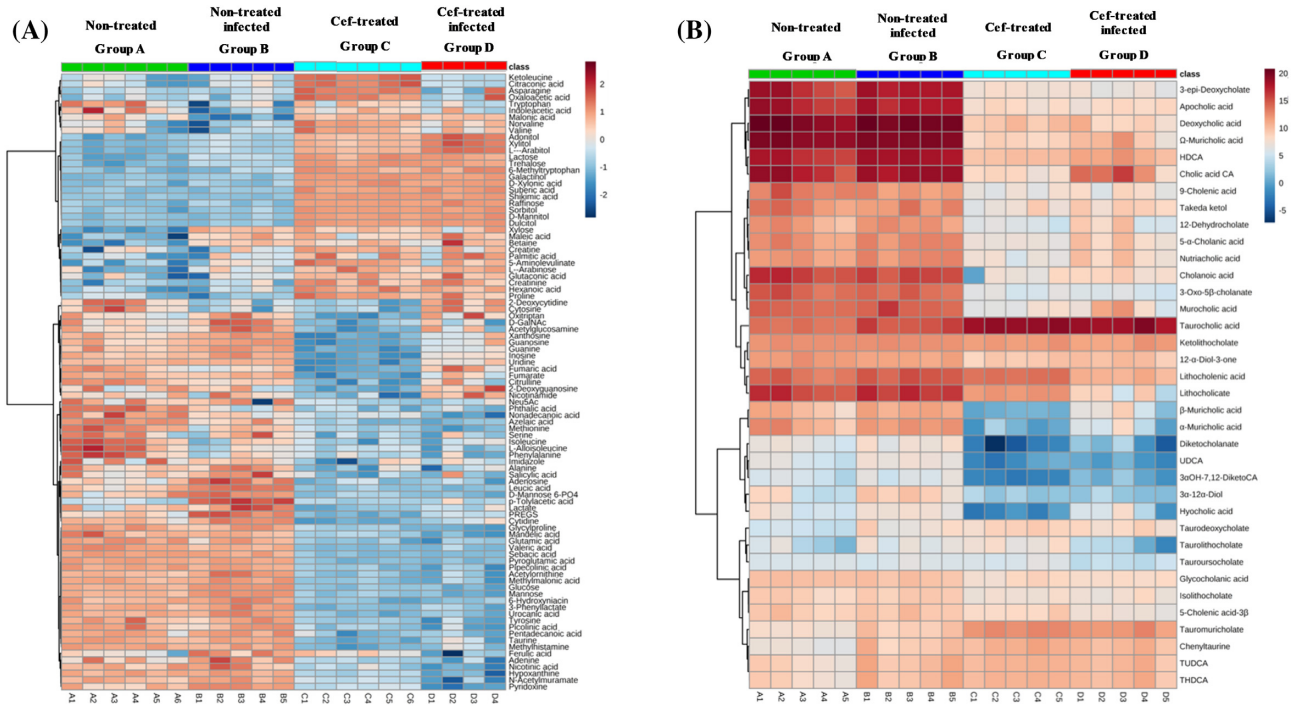

Figure 2. Targeted metabolomics of cecal metabolome. Heatmap of the metabolites grouped by KEGG pathway **(A)** and bile acids **(B)** found in the non-treated and cef-treated groups infected with or without *C. albicans* are shown. The heatmap scale ranges from −2 to 2 (KEGG pathway metabolites) and −5 to 20 (bile acids) on a $\log_2$ scale. Group of 4 to 6 mice were used in each group.

treated mice infected with this fungi (Fig. 2A and Figure S2, Supporting Information).

Conjugated bile acids such as taurocholic acid (TCA), taurolithocholic acid (TLCA), taurodeoxycholic acid (TDCA), tauromurocholic acid (TMCA), taurohyodeoxycholic acid (THDCA), tauroursodeoxycholic acid (TUDCA) showed a significant increase, while secondary bile acids including deoxycholic acid (DCA), hyodeoxycholic acid (HDCA), ursodeoxycholic acid (UDCA), lithocholic acid (LCA), murocholic acid (MCA), cholic acid (CA) and cholenic acid derivatives levels decreased in cef-treated mice (Fig. 2B; Figures S2 and S3 Data, Supporting Information). Interestingly, the cef-treated group (Group D) infected with *C. albicans* showed a considerable increase in cholic acid and hyocholic acid levels (Fig. 2B and Figure S2, Supporting Information). In conclusion, a diverse array of derivatized fatty acids, and bile acids, became significantly altered via cefoperazone treatment. Further infection with *C. albicans* in the cefoperazone treated mice considerably effected the composition of these metabolites.

Gut metabolites differentially regulate the growth of *C. albicans in vitro*

To define the relationship between relevant *in vivo* levels of gut metabolites in the cecal contents of cef-treated mice and *C. albicans* colonization of their GI tracts, we tested the effect of gut metabolites on *C. albicans* growth *in vitro*. Major metabolite groups including carbohydrates, sugar alcohols, carboxylic acids and bile acids that are predominantly different between non-treated and cef-treated groups were validated *in vitro* to determine their effects on *C. albicans* growth.

Carbohydrates including glucose and mannose had the largest impact on *C. albicans* growth. Glucose and mannose significantly increased the growth of this fungi by more than 1000% compared to YNB media containing vehicle (Fig. 3A). Mannitol, sorbitol, xylose, adonitol and xylitol also significantly increased the growth of *C. albicans* (100–200%) compared to vehicle control (Fig. 3A). Other metabolites including raffinose, arabinose, trehalose, lactose, galactinol, galactitol and arabitol had little or marginal impact on *C. albicans* growth (Fig. 3A).

Carboxylic acids showed an inhibitory effect on the growth of *C. albicans*. Salicyclic, p-tolyacetic, lactic acid and sebacic acid completely inhibited the growth of this fungi (Fig. 3B). 2-methylbutyric, picolinc, methylmalonic and fumaric acid significantly inhibited the growth of *C. albicans* by more than 75%, relative to the vehicle. Azelaic, palmitic, glutaconic, n-acetylmuramic, leucic and pentadeconoic acid all displayed 50–75% inhibition compared to vehicle. Shikimic, suberic, pipecolinic and n-acetylneuraminic acids had marginal or no effect on the growth of this fungi at the concentrations used in this study (Fig. 3B).

Bile acids showed a mixed trend. Conjugated bile acids promoted, whereas unconjugated secondary bile acids inhibited the growth of *C. albicans* (Fig. 3C). TCA, TCDCA and CDCA significantly increased the growth by 30–50%, relative to vehicle control. DCA, i-DCA, LCA and i-LCA showed potent inhibition (70%) relative to vehicle control. HDCA and UDCA also significantly inhibited *C. albicans* growth by 20 to 30%. CA, TLCA, GCA and TDCA showed little or marginal effect at the concentrations used in this study (Fig. 3C). Taken together, we found carbohydrates and sugar alcohols promoted growth, carboxylic acids inhibited growth, while bile acids had differential effects on *C. albicans* growth *in vitro*.

Gut metabolites differentially regulate the *C. albicans* hyphae formation *in vitro*

The morphological transition from yeast to hyphae is a key determinant in the virulence potential of *C. albicans*. Therefore, inhibition of the morphological plasticity of *C. albicans* would

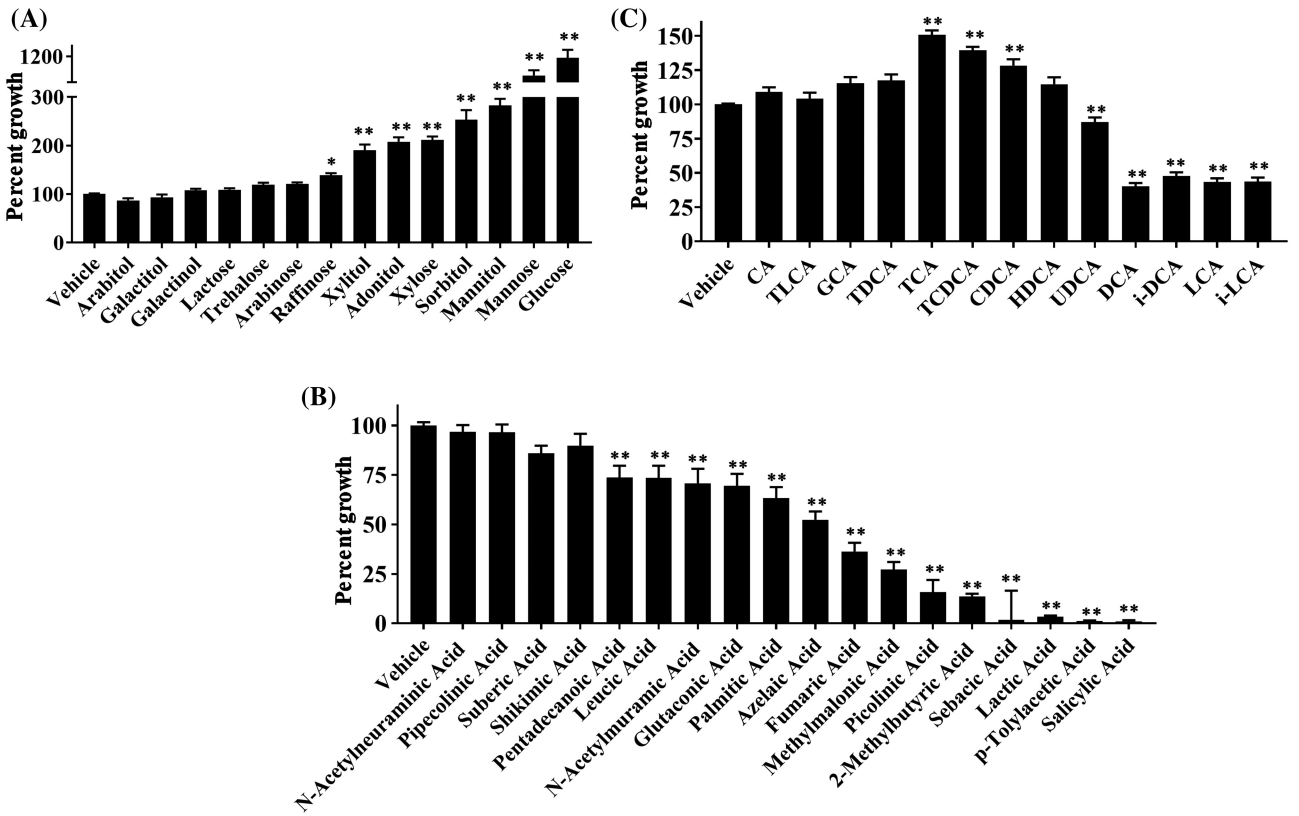

Figure 3. Gut metabolites differentially regulate the growth of *C. albicans*. Growth of *C. albicans* SC5314 incubated in the presence or absence of indicated carbohydrates **(A)**, carboxylic acids **(B)** and bile acids **(C)** was determined by spectrophotometer at an optical density of 600 nm. Gut metabolites were tested using different growth media as detailed in the methods section and appropriate vehicles (water or DMSO or ethanol) were used for their respective control groups. Carbohydrates were tested at 5 mg/mL. Carboxylic acids (suberic acid, picolinic acid, pipecolinic acid and shikimic acid [0.1 mg/mL]; 2-methylbutyric acid, glutaconic acid, n-acetylmuramic acid and n-acetylneuraminic acid [0.5 mg/mL]; lactic acid [5 mg/mL]); pentadecanoic acid [0.025 mg/mL]; fumaric acid, methylmalonic acid, palmitic acid, leucic acid, p-tolylacetic acid and salicylic acid [0.5 mg/mL]; sebacic acid and azelaic acid [0.5 mg/mL]); and urocanic acid [0.1 mg/mL]) were tested at the indicated concentrations. Bile acids: LCA and iLCA (0.1 mg/mL); DCA, HDCA and UDCA (0.5 mg/mL); iDCA (0.25 mg/mL); GCA, TCA, TCDCA and TLCA (0.1 mg/mL); CA, CDCA and TDCA (0.5 mg/mL) were used at these concentrations. Experiment was repeated three times and the three combined replicates are shown here. Data is represented as mean ± SEM. Statistical significance was evaluated using students t-test and *P* values ($^{*} \leq 0.05$, $^{**} \leq 0.01$) were considered as significant.

substantially reduce its pathogenic potential, including host cell penetration and tissue damage (Lo *et al.* 1997; Toenjes *et al.* 2005; Fazly *et al.* 2013; Bar-Yosef *et al.* 2017; Vila *et al.* 2017). A variety of factors in the gut, including n-acetylglucosamine and bacterial peptidoglycan, regulate hyphal formation by *C. albicans* (Piispanen and Hogan 2008; Xu *et al.* 2008; Naseem *et al.* 2011). Therefore, we investigated the effect of gut metabolites on *C. albicans* hyphae formation.

Molecular classes belonging to carbohydrates, sugar alcohols, carboxylic acids and bile acids were tested for their effect on *C. albicans* hyphae development. Preliminary screening was carried out in YNB or RPMI + FBS medium to identify if metabolites promoted or inhibited hyphae formation. *Candida albicans* grown in YNB media incubated at 37°C for about 3 to 4 hours usually do not form hyphae. However, fungal cells grown in nutrient rich RPMI media containing 30% FBS form massive hyphae in 3 to 4 hours of incubation at 37°C. These different growth conditions were used to examine the effect of metabolites on hyphae formation. Interestingly, our results indicate that gut metabolites differentially regulate hyphae formation (Figure S4–6, Supporting Information).

Metabolites such as xylitol, mannitol, TLCA, TDCA, TCA, TCDCA, mannose and glucose significantly promoted *C. albicans* hyphae formation in YNB media compared to control group (Fig. 4A). TLCA, TDCA, mannose and glucose induced hyphae, pseudohyphae, or germ tube like structures in about 5–10% of fungal cells (Fig. 4B). Xylitol, TCA and TCDCA also significantly induced hyphae like bodies in about 3–4% of fungal cells within the short incubation period of 3–4 hours (Fig. 4B).

On the other hand, metabolites such as sebacic, palmitic, p-tolyacetic, 2-methylbutyric, salicylic acid, CA, HDCA, UDCA, LCA, i-LCA, DCA and i-DCA significantly inhibited the hyphae development relative to the control group (Fig. 5A). *Candida albicans* formed massive hyphae in the presence of FBS and more than 90% of fungal cells exhibited hyphae development in the control group (Fig. 5A and B). Interestingly, metabolites including sebacic, palmitic, p-tolyacetic, 2-methylbutyric, salicylic acid, CA, HDCA, UDCA, LCA, i-LCA, DCA and i-DCA significantly inhibited the hyphae development even in the presence of FBS compared to control group. Only less than 5% of fungal cells developed hyphae in the presence of these metabolites (Fig. 5A and B). However, no appreciable impact on *C. albicans* hyphae development was observed with other gut metabolites at the concentrations used in this study (Figure S4–6, Supporting Information). Collectively, gut metabolites differentially regulate the hyphae formation in *C. albicans*.

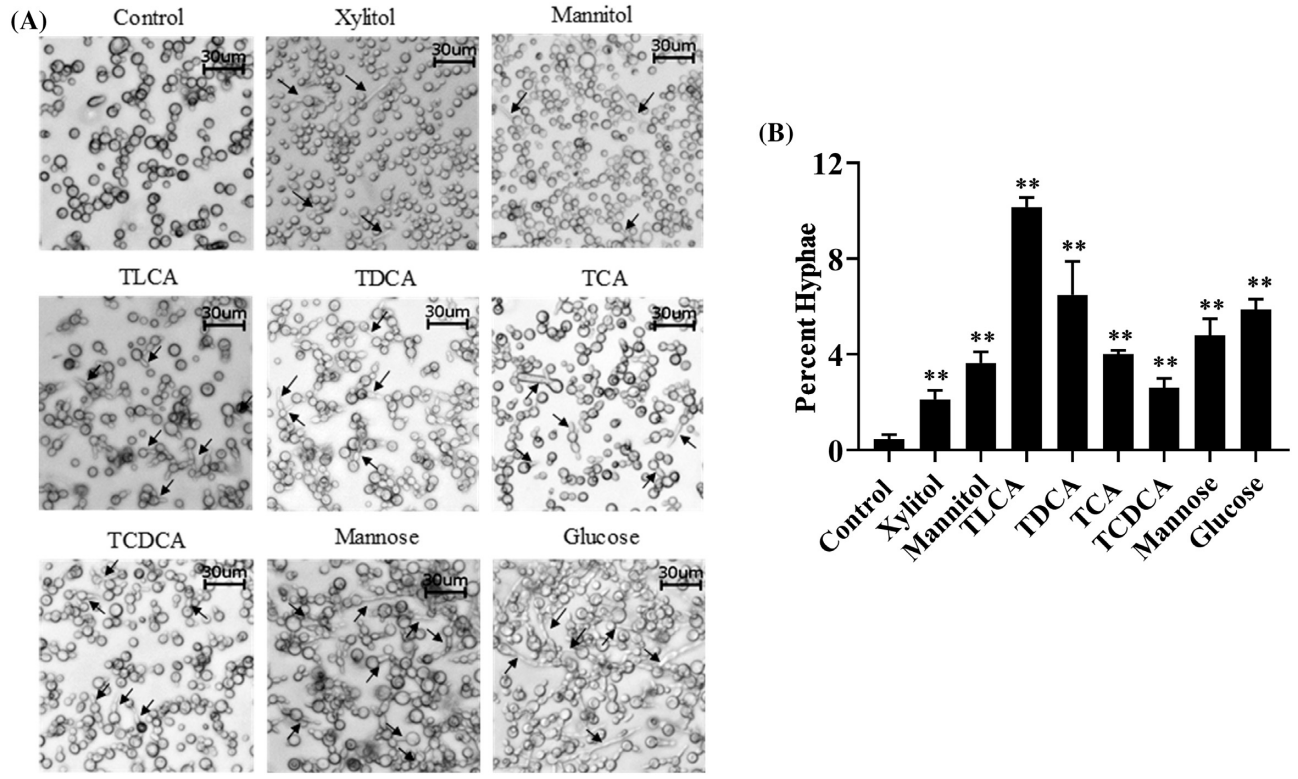

Figure 4. Gut metabolites promote *C. albicans* hyphae formation. **(A)** *Candida albicans* SC5314 incubated in the presence or absence of indicated metabolites and the hyphal formation imaged at 40X using Keyence BZ-X700 microscope. Representative images are shown here. Control group was grown in YNB media, and treatment groups were grown in the presence of indicated gut metabolites in YNB media as detailed in the methods section. **(B)** Percent hyphae in the presence or absence of indicated gut metabolites were determined. Atleast 5 images were counted per group. Data represented as means ± SEM. Statistical significance was evaluated using students t-test and *P* values (* ≤ 0.05, ** ≤ 0.01) were considered as significant.

Correlations between the cecal metabolome and microbiome

Given that antibiotic treatment alters the composition of gut microbiome, and the microbiome plays a significant role in regulating the GI metabolic environment (Sridharan *et al.* 2014; Theriot *et al.* 2014) and colonization of *C. albicans* (Fan *et al.* 2015), we examined if antibiotic induced changes in the composition of the gut metabolome correlates to the changes in the microbiome. Correlating the changes between metabolome and microbiome may provide insight into the metabolic function of the microbiome, and thus could act as a potential link for further investigation to elucidate mechanisms of *C. albicans* colonization after antibiotic use.

We examined the composition of the bacterial gut microbiome in the non-treated and cef-treated mice using 16S ribosomal RNA amplicon gene sequencing. At phyla-level, relative abundance of Firmicutes was considerably higher, whereas relative abundance of Bacteroidetes and Verrucomicrobia were lower in cef-treated groups than in non-treated mice (Fig. 6A). At the family-level, relative abundance of Panibacillaceae was higher, whereas the relative abundance of Lactobacillaceae, Turicibacteraceae, Clostridiales and Clostridiaceae was lower in cef-treated mice (Fig. 6B). Next, we examined if infection with *C. albicans* on these groups had any impact on the gut bacterial community. Non-treated adult mice infected with *C. albicans* had little impact on phyla and family-level abundance (Figs 6A and 6B). Cef-treated mice infected with *C. albicans* had a significant shift in their bacterial composition. Firmicutes was the major phyla observed in the cef-treated mice, whereas infection with *C. albicans* lead to an increased relative abundance of Proteobacteria (75%) and Cyanobacteria (20%) members (Fig. 6A). At family-level, higher relative abundance in Verrucomicrobiaceae, Rickettsiales and Proteobacteria members were observed with *C. albicans* infection (Fig. 6B). Kruskal–Wallis pairwise comparison was used to determine statistical significance (*P* value ≤ 0.05). As seen in the Supplementary Figure 8 (Supporting Information), *C. albicans* (Group B) alone had no significant impact on diversity relative to the control treatment (Group A) as measured by Faith's Phylogenetic Diversity index. However, Cef-treated mice infected with *C. albicans* (Group D) had significantly higher bacterial diversity relative to all other treatments.

We also determined the relative abundance of OTUs in all the four groups (Fig. 6C). Non-treated groups had similar high abundance OTUs. These OTUs included the S24–7 family, the genera Allobaculum, Lactobacillus and Turicibacter, and the species *Akkermansia municiphila*. Cef-treated group was enriched in the genus Paenibacillus, a known pathogen that accounted for over 90% of detected OTUs. *Candida albicans* infection in the cef-treated group had fewer high abundance OTUs relative to other three groups. The most abundant OTUs in this group were unclassified Proteobacteria, the orders Streptophyta and Rickettsiales, the genera Achromabacter, a known pathogen, and Burkholderia (Fig. 6C).

Next, we examined the correlation between the bacterial microbiome and KEGG metabolites including carbohydrates, sugar alcohols and carboxylic acids in the different groups using Spearman's rank correlation analysis. As opposed to controls (Group A), phyla including Bacteroidetes, Verrucomicrobia, Firmicutes and Actinobacteria in the cef-treated (Group C)

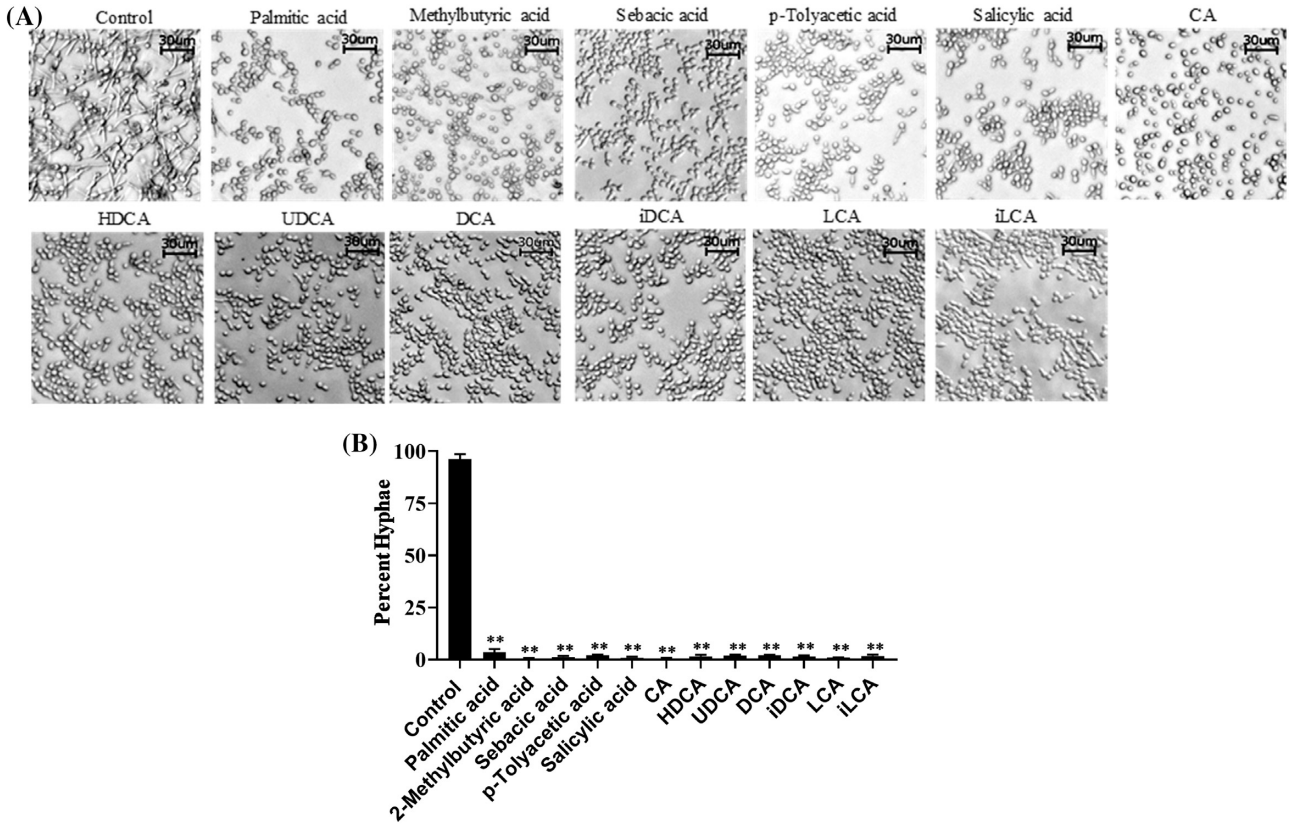

Figure 5. Gut metabolites inhibit *C. albicans* hyphae formation. **(A)** *Candida albicans* SC5314 incubated in the presence or absence of indicated metabolites and the hyphal formation imaged at 40X using Keyence BZ-X700 microscope. Representative images are shown here. Control group was grown in RPMI media containing 30% FBS, and treatment groups were grown in the presence of indicated gut metabolites in RPMI media containing 30% FBS as detailed in the methods section. **(B)** Percent hyphae in the presence or absence of indicated gut metabolites were determined. Atleast 5 images were counted per group. Data represented as means ± SEM. Statistical significance was evaluated using students t-test and *P* values ($^{*} \leq 0.05$, $^{**} \leq 0.01$) were considered as significant.

were positively correlated with the majority of carbohydrates and sugar alcohols (Fig. 6D). Similarly, phyla including Actinobacteria, Bacteroidetes and Verrucomicrobia showed a positive correlation with carboxylic acids including glutaconic acid, n-acteylmuramic acid, pentadeconoic acid, salicyclic and p-tolyacetic acids in the cef-treated group. A smaller degree of correlation between carboxylic acids and phyla was seen in the control groups. Phylum Firmicutes in the antibiotic treated group was positively correlated with 2-methylbutyric acid (Fig. 6E). Significant correlations were seen across metabolites spanning sugar and carboxylic acid derivatives across all cohorts examined (S7 Data, Supporting Information). These results indicate that changes in the levels of certain cecal metabolites that regulate the growth and morphogenesis of *C. albicans* were associated with changes in gut microbiome composition.

Predictive 16S rRNA gene function and putative gene category markers across all four cohorts

Inferred gene products and their pathways determined by PICRUSt were categorized into metabolic compartments to survey predicted gene functions differentially abundant across the cefoperazone treated and control groups with and without *C. albicans* infection. An LDA score was computed for each of these functions using LEfSe—both algorithms were utilized in tandem from the Galaxy server hosted on the Huttenhower laboratory website. A total of 153 of these compartmentalized gene functions were deemed statistically significant according to LDA scores and were thus focused for additional analysis. Plotting the normalized PICRUSt gene family counts as heatmaps revealed several hot spots for group C (cefoperazone treated mice) that qualitatively contrasted from the other groups (A, B and D). OTU counts mapping to carbohydrate metabolism, nucleotide metabolism and bacterial cell wall metabolism were found to be enhanced in the Group C cohort (Fig. 7 and Figure S9, Supporting Information). Specifically, LEfSe pointed to sugar pathways (both catabolic and anabolic) for energy metabolism of alternative glycolytic forms: fucose, mannan and hexitol degradation were deemed as markers for this cohort (Fig. 7A and B). Both salvage and *de novo* pyrimidine and purine pathways were seen as potential markers from Group C. Sulfur and formaldehyde metabolism, urea cycle components were also preferentially delineated as group C markers (Fig. S9, Supporting Information).

Contrasting with Group C, bacterial cell wall development, regulation and metabolism (O-antigen synthesis, peptidoglycan maturation and LPS associated functional genes) were markers across all groups (Fig. 7A and Figure S9, Supporting Information). While peptidoglycan, a cell wall component ubiquitous in both Gram negative and positive bacteria, was predicted to be enriched in all Groups, a statistically significant LDA score for Group D (cefoperazone treated mice infected with *C. albicans*) was found by the LEfSe pipeline for gene products encoding LPS (lipopolysaccharide) synthesis (Fig. 7A and Figure S9, Supporting Information). This could be evidential of the dual effects of cefoperazone perturbation with the presence of

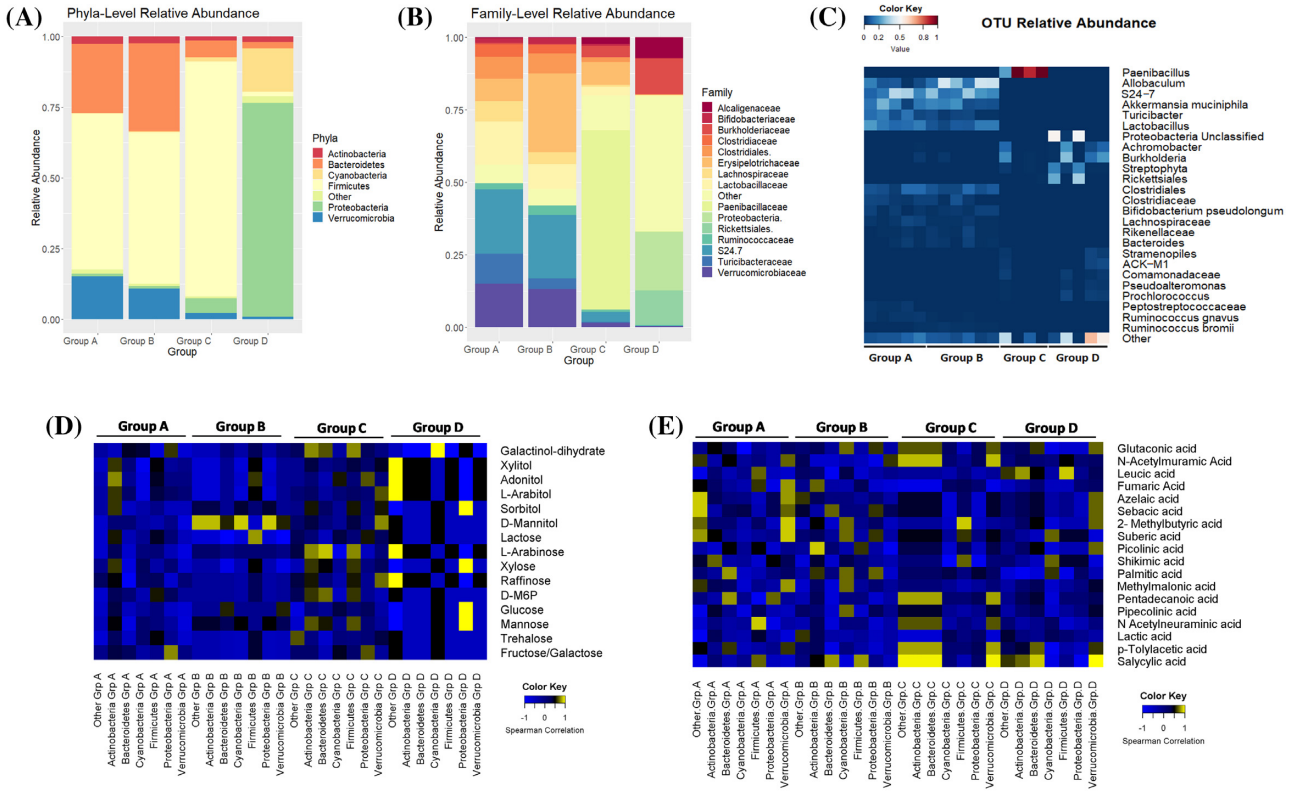

Figure 6. Correlations between the cecal metabolome and microbiome. Relative abundance of major phyla **(A)** and family **(B)** in the four groups: non-treated (Group A), non-treated infected with *C. albicans* (Group B), cef-treated (Group C) and cef-treated infected with *C. albicans* (Group D) were shown here. Group of 5 mice were used in each group. **(C)** Relative abundances of 26 high abundance (>1%) OTUs for all treatment groups are displayed as a heatmap. The relative abundances for all 402 detected OTUs were calculated. OTUs with low abundance (<1%) across all groups were filtered into the 'Other' category. The OTU relative abundance scale ranges from 0 to 100% abundance. **(D)** Heatmap visualization showing spearman correlation values of top 15 metabolites belonging to carbohydrates with phylum OTUs. Spearman correlates were stratified according to Groups. D-M6P stands for D-mannose-6-phosphate. **(E)** Spearman correlation values of top 18 carboxylic acid metabolites correlated with phylum OTUs.

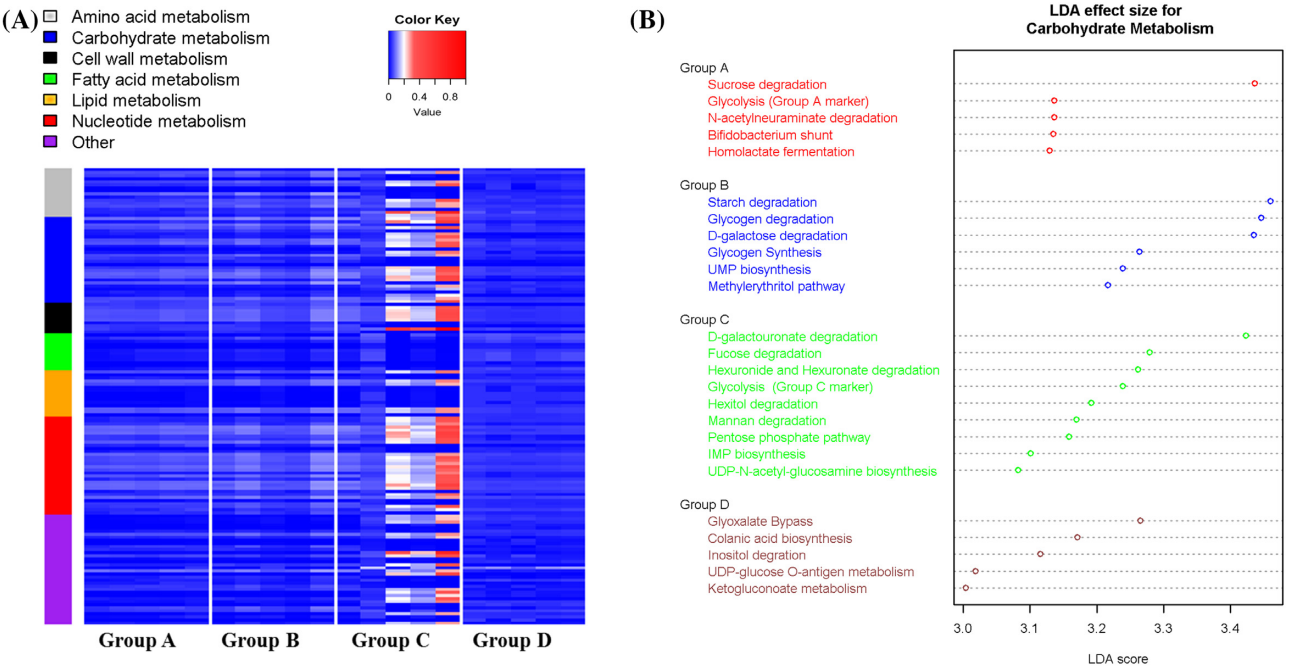

Figure 7. **(A)** Heatmap of PiCRUST output normalized so that OTU gene families across all samples vary from 0 to 1. Predicted gene functionalities were grouped into one of 7 categories as shown by the colored row bars. **(B)** Dot plots of categorized gene OTU functions inferred from PiCRUST. Statistically significant LDA scores ($P < 0.05$, based on LEfSe's Wicoxon test) are plotted. Statistically significant LDA scores >3.0 were plotted as the arbitrary cutoff.

Candida—making the cecal microbiota more prone to gene products associated with pathogenic bacteria. In cell model systems, LPS and *Candida* cell wall portions have been shown to synergistically promote the activation of the macrophage line RAW264.7 causing inflammation and elevated host immune responses (Bie *et al*. 2019). Translating these findings to the cecum model employed in this study, it can be considered that the pathogenic insult of *Candida*, combined with dysbiosis caused by cefoperazone, favors the Group D cohort to harbor bacterial niches that optimize in secreting LPS layers—a known inflammation protagonist. Finally, Group D mice were shown by LEfSe to be preferentially enriched in genes products encoding fatty acid metabolism (synthesis, degradation and elongation) (Fig. 7A and Figure S9, Supporting Information). The enhanced fatty acid metabolic profile in Group D may reflect a change in either the gut flora constituents from cefoperazone administration or alterations originating from *Candida* insult.

The predicted functional data from PICRUSt highlight areas of convergence when compared to our generated LC-MS metabolomics data. First, the LC-MS data in Figure 6D highlights the high correlation witnessed between alternative sugar metabolism (particularly xylitol, adonitol and L-arabitol) with microbiome phyla. Likewise, the presence of many sugar metabolic genes (particularly those outside of canonical glucose metabolism) was inferred from 16S OTU gene families from PICRUSt in Group C. Fatty acids were also found abundant on our metabolomics dataset, albeit from both Group C and Group D, as seen in the hotspots in the Figure 6E heatmap; convergently, an array of fatty acid compounds were predicted by PICRUSt to be markers in both cefoperazone treated groups (Figure S9, Supporting Information). The heatmap addressing metabolome coverage (Fig. 2) shows primary nucleotide metabolism being enhanced in Group A and Group B controls. This was also seen in the predicted gene content for these two control cohorts as well. Figure 7 and Supplementary Figure 9 (Supporting Information) reveals statistically significant LDA scores for adenosine, guanosine, purine degradation and CDP metabolism. Our metabolome data for the control groups coincides and validates these *in-silico* findings. As a whole, predicted functional data at the 16S level highlighted areas of convergence with metabolites witnessed from the LC-MS metabolomics screen—primarily with carbohydrates and nucleotides. Despite this, the exact origin and characterization of microbiome genes and their relationships to specific metabolites merits further work.

DISCUSSION

Since antibiotics have been shown to have a profound impact on the gut ecosystem, a multi-omics approach combined with follow up *in-vitro* experiments were utilized to better understand the changes in the cecal metabolome and microbiome within the context of *C. albicans* infection. The ability of the gut microbiome to suppress pathogenic organisms has been studied for the past few decades (Bohnhoff, Drake and Miller 1954; Kennedy and Volz 1985; Wiesner *et al*. 2001; Kim *et al*. 2017). Gut microbiota control the pathogenesis of enteric pathogens—collectively termed 'colonization inhibition'—through several mechanisms that include modulating host immune response, outcompeting pathogenic organisms for nutrients, direct interactions between gut microbiota and pathogens, and through the production of metabolites (Buffie and Pamer 2013; Theriot *et al*. 2014; Fan *et al*. 2015; Neville, d'Enfert and Bougnoux 2015; Kim, Covington and Pamer 2017; Allonsius *et al*. 2019). Profound documented evidence exists suggesting that gut metabolites secreted by commensal microbiota help in establishing colonization resistance to enteric pathogens (Young and Schmidt 2004; Dethlefsen and Relman 2011; Theriot *et al*. 2014; Weingarden *et al*. 2014; Buffie *et al*. 2015; Fan *et al*. 2015; Theriot, Bowman and Young 2016; Lustri, Sperandio and Moreira 2017; Suez and Elinav 2017; Guinan and Thangamani 2018; Guinan, Villa and Thangamani 2018; Kohli *et al*. 2018; Seekatz *et al*. 2018; Thangamani *et al*. 2018). In this study, we examined if gut metabolites regulate the GI colonization of *C. albicans* by determining the effect of cecal metabolites on *C. albicans* growth and morphogenesis. We found that antibiotic treatment resulted in an observable shift in the levels of bile acids, carbohydrates, carboxylic acids and sugar alcohols, all of which predispose *C. albicans* growth and morphogenesis. The changes in *C.albicans* morphology in the presence of these metabolites were affirmed microscopically and through growth assays. Bacterial products such as carboxylic acids and secondary bile acids are elevated in the baseline metabolome, whereas these metabolites were largely lower in comparison after antibiotic treatment. Bacterial substrates such as carbohydrates, sugar alcohols and primary bile acids were significantly elevated with cefoperazone treatment. *In vitro*, we confirmed that carbohydrates, sugar alcohols and primary bile acids promote, whereas carboxylic acids and secondary bile acids inhibit the growth and morphogenesis of *C. albicans*. Previously, we reported that levels of SCFAs and certain bile acids are altered with cefoperazone treatment and facilitate *C. albicans* growth and morphogenesis (Guinan and Thangamani 2018; Guinan, Villa and Thangamani 2018; Thangamani *et al*. 2018). This study along with our previous findings indicate that alterations at the levels of gut metabolites resulting from antibiotics correlate to the increased growth and hyphae formation of *C. albicans* in the GI tract. It is worth noting that *in-vitro* growth and hyphae experiments in this study were performed in the presence of ambient levels of oxygen. Oxygen level in the GI tract varies disproportionately (Friedman *et al*. 2018) and hypoxia itself influences filamentation patterns of fungi (Setiadi *et al*. 2006; Synnott *et al*. 2010; Desai *et al*. 2015). Stomach and duodenum are considered highly oxygenated environments, whereas ileum and cecum are anaerobic under healthy conditions (Friedman *et al*. 2018). Emerging evidences indicate that antibiotic treatment leads to increased oxygen levels in the gut lumen, creating a permissive environment for enteric pathogens to utilize substrate oxygen to express virulence factors, and exponentially colonize the gut (Marteyn *et al*. 2010; Kelly *et al*. 2015; Byndloss *et al*. 2017; Mullineaux-Sanders *et al*. 2018; Reese *et al*. 2018; Yoon and Yoon 2018). Additionally, other factors including temperature, pH, antifungal peptides and direct interaction with commensal bacteria impact *C. albicans* growth and morphogenesis (Shirtliff, Peters and Jabra-Rizk 2009; Vylkova *et al*. 2011; Martin *et al*. 2013; Desai *et al*. 2015; Neville, d'Enfert and Bougnoux 2015; Allonsius *et al*. 2019; Hager *et al*. 2019). Results from this study form a strong basis for future studies to investigate how gut metabolites differentially regulate the growth and hyphae formation of *C. albicans* under conditions that *C. albicans* encounters during growth in the mammalian GI tract. Quantifying the metabolites concentration in the gut contents from control and cef-treated mice are also important to gain more insights into the concentration dependent effect of gut metabolites on *C. albicans* growth and morphogenesis *in vivo*.

Using a Spearman rank coefficient, a significant correlation between the changes in gut metabolite levels and microbiome composition conducive to *C. albicans* was also found in this study. A relative decrease in the abundance of Bacteroidetes

correlated to increased levels of carbohydrates and sugar alcohols observed in the antibiotic-treated groups. Bacteroidetes phyla are efficient at utilizing carbohydrates and sugar alcohols in their environment (Hooper, Midtvedt and Gordon 2002; Wexler 2007) and this observation may be the phenomenon we are witnessing here. These bacteria are capable of utilizing simple and complex sugars found in the intestine, which was illustrated by the high prevalence of paralogous proteins for carbohydrate uptake and degradation in these species (Hooper, Midtvedt and Gordon 2002; Wexler 2007). A relative decrease in Lactobacillacaeae and Clostridiales also correlated to an increase in the levels of primary bile acid metabolites, and concomitantly, a decrease in secondary bile acids in the cecum of antibiotic treated mice. Conjugated primary bile acids secreted into the small intestine are catalyzed by bile salt hydrolases (BSHs) from gut bacteria, mainly by members of Lactobacillacaeae in the ileum (Begley, Hill and Gahan 2006; Ridlon, Kang and Hylemon 2006; Ridlon, Kang and Hylemon 2006; Ridlon and Hylemon 2012; Ridlon *et al.* 2014; Wahlstrom *et al.* 2016; Ramirez-Perez *et al.* 2017; O'Flaherty *et al.* 2018). Unconjugated primary bile acids are further metabolized to secondary bile acids by only a few anaerobic bacteria in the cecum, largely represented by *Clostridium scindens* and other *Clostridium spp.* (Ridlon, Kang and Hylemon 2006; Ridlon and Hylemon 2012; Ridlon *et al.* 2014; Ridlon *et al.* 2016; Wahlstrom *et al.* 2016; Ramirez-Perez *et al.* 2017). The presence of these secondary bile acids, created by specific gut flora, seem essential for maintenance of a healthy host. Deprivation of these compounds either via antibiotic dysbiosis may facilitate a niche for *C. albicans*. The recapitulation of some of these bile acids into *Candida albicans* growth media seem was shown to decrease the percentage growth of the fungi. Furthermore, recent studies indicate that gut commensal bacteria have the potential to create a diverse array of natural products, as evidenced by the presence of large biosynthetic gene clusters (BGCs) involved in various metabolite production (Donia *et al.* 2014; Bratburd *et al.* 2018). Therefore, future studies to characterize the BGCs involved in metabolite production are essential to modulate the gut ecosystem in human health and diseases—the lack of which can serve as fertile ground for pathogenic fungi to preponderate.

While analysis of the gut microbiota has focused predominantly on bacterial components, the mycobiome has emerged as an important player in the gut ecosystem. Therefore, in this study, we also examined if *C. albicans* infection alters the gut metabolites and bacterial microbiome composition in the non-treated and antibiotic treated adult mice. Interestingly, we found that the relative abundance of bacterial microbiome and metabolites were not considerably altered upon infection with *C. albicans* in the non-treated control groups (Group B). However, relative abundance of Proteobacteria which is mostly comprised of several pathogenic bacteria including Rickettsia, Bordetella, Escherichia, Shigella and Salmonella were significantly increased in the cef-treated infected mice (Group D) (Shin, Whon and Bae 2015; Bradley and Pollard 2017; Rizzatti *et al.* 2017). A previous study by Mason *et al.* also indicates that presence of this fungi in the antibiotic-treated mice decreased the abundance of Lactobacillus, whereas increased the *Enterococcus faecalis* population (Mason *et al.* 2012). In addition, presence of *C. albicans* also reduced the efficacy of fecal microbiota transplantation for *C. difficile* treatment (Zuo *et al.* 2018). On the other hand, a recent study demonstrated that gut evolved strains of *C. albicans* confer protective immunity against various bacterial and fungal pathogens to the host (Tso *et al.* 2018). Although it is apparent that shifts may occur in the microbiome and metabolome composition in response to *C. albicans*, future studies to investigate the role of *C. albicans* on gut ecosystem in a healthy and dysbiotic state, and identify the known and unidentified metabolites in these settings are essential to gain insights into their roles in the gut and human health (Bratburd *et al.* 2018).

SUPPLEMENTARY DATA

Supplementary data are available at FEMSEC online.

ACKNOWLEDGEMENTS

This work was supported by Midwestern University faculty start-up fund and intramural research awards to Dr. Thangamani. The authors acknowledge resources and support from the Genomics Core, part of the Biosciences Core Facilities at Arizona State University.

Conflict of interest. None declared.

REFERENCES

Allonsius CN, Vandenheuvel D, Oerlemans EFM *et al.* Inhibition of *Candida albicans* morphogenesis by chitinase from *Lactobacillus rhamnosus* GG. *Sci Rep* 2019;**9**:2900.

Bar-Yosef H, Vivanco Gonzalez N, Ben-Aroya S *et al.* Chemical inhibitors of *Candida albicans* hyphal morphogenesis target endocytosis. *Sci Rep* 2017;**7**:5692.

Begley M, Hill C, Gahan CG. Bile salt hydrolase activity in probiotics. *Appl Environ Microbiol* 2006;**72**:1729–38.

Bendel CM, Kinneberg KK, Jechorek RP *et al.* Effects of alteration of the *Candida albicans* gene *int1* on cecal colonization in orally innoculated mice. *Pediatr Res* 1999;**45**:156A.

Berlanga M, Palau M, Guerrero R. Gut microbiota dynamics and functionality in *Reticulitermes grassei* after a 7-day dietary shift and ciprofloxacin treatment. *PLoS One* 2018;**13**:e0209789.

Bie X, Zhang S, Luo X *et al. Candida albicans* cell wall mannoprotein synergizes with lipopolysaccharide to affect RAW264.7 proliferation, phagocytosis and apoptosis. *Microb Pathog* 2019;**131**:98–105.

Bohm L, Torsin S, Tint SH *et al.* The yeast form of the fungus *Candida albicans* promotes persistence in the gut of gnotobiotic mice. *PLoS Pathog* 2017;**13**:e1006699.

Bohnhoff M, Drake BL, Miller CP. Effect of streptomycin on susceptibility of intestinal tract to experimental *Salmonella* infection. *Proc Soc Exp Biol Med* 1954;**86**:132–7.

Bradley PH, Pollard KS. Proteobacteria explain significant functional variability in the human gut microbiome. *Microbiome* 2017;**5**:36.

Bratburd JR, Keller C, Vivas E *et al.* Gut microbial and metabolic responses to *Salmonella enterica* serovar typhimurium and *Candida albicans*. *MBio* 2018;**9**:02032-18.

Buas MF, Gu H, Djukovic D *et al.* Candidate serum metabolite biomarkers for differentiating gastroesophageal reflux disease, Barrett's esophagus, and high-grade dysplasia/esophageal adenocarcinoma. *Metabolomics* 2017;**13**:11306-016-1154-y.

Buffie CG, Pamer EG. Microbiota-mediated colonization resistance against intestinal pathogens. *Nat Rev Immunol* 2013;**13**:790–801.

Buffie CG, Bucci V, Stein RR *et al.* Precision microbiome reconstitution restores bile acid mediated resistance to *Clostridium difficile*. *Nature* 2015;**517**:205–8.

Byndloss MX, Olsan EE, Rivera-Chavez F *et al.* Microbiota-activated PPAR-gamma signaling inhibits dysbiotic Enterobacteriaceae expansion. *Science* 2017;**357**:570–5.

Caporaso JG, Lauber CL, Walters WA *et al.* Global patterns of 16S rRNA diversity at a depth of millions of sequences per sample. *Proc Natl Acad Sci USA* 2011;**108**:4516–22.

Caporaso JG, Kuczynski J, Stombaugh J *et al.* QIIME allows analysis of high-throughput community sequencng data. *Nat Methods* 2010;**7**:335–6.

Carlisle PL, Banerjee M, Lazzell A *et al.* Expression levels of a filament-specific transcriptional regulator are sufficient to determine *Candida albicans* morphology and virulence. *Proc Natl Acad Sci USA* 2009;**106**:599–604.

Carroll PA, Diolaiti D, McFerrin L *et al.* Deregulated Myc requires MondoA/Mlx for metabolic reprogramming and tumorigenesis. *Cancer Cell* 2015;**27**:271–85.

Chong J, Soufan O, Li C *et al.* MetaboAnalyst 4.0: towards more transparent and integrative metabolomics analysis. *Nucleic Acids Res* 2018;**46**:W486–94.

Chu Y, Jiang MZ, Xu B *et al.* Specific changes of enteric mycobiota and virome in inflammatory bowel disease. *J Dig Dis* 2018;**19**:2–7.

Cole GT, Halawa AA, Anaissie EJ. The role of the gastrointestinal tract in hematogenous candidiasis: from the laboratory to the bedside. *Clin Infect Dis* 1996;**22**:S73–88.

Delaloye J, Calandra T. Invasive candidiasis as a cause of sepsis in the critically ill patient. *Virulence* 2014;**5**:161–9.

Desai PR, van Wijlick L, Kurtz D *et al.* Hypoxia and temperature regulated morphogenesis in *Candida albicans*. *PLoS Genet* 2015;**11**:e1005447.

Dethlefsen L, Relman DA. Incomplete recovery and individualized responses of the human distal gut microbiota to repeated antibiotic perturbation. *Proc Natl Acad Sci USA* 2011;**108**:4554–61.

Donia MS, Cimermancic P, Schulze CJ *et al.* A systematic analysis of biosynthetic gene clusters in the human microbiome reveals a common family of antibiotics. *Cell* 2014;**158**:1402–14.

Enaud R, Vandenborght LE, Coron N *et al.* The mycobiome: a neglected component in the microbiota-gut-brain axis. *Microorganisms* 2018;**6**:1-13.

Fan D, Coughlin LA, Neubauer MM *et al.* Activation of HIF-1alpha and LL-37 by commensal bacteria inhibits *Candida albicans* colonization. *Nat med* 2015;**21**:808–14.

Fazly A, Jain C, Dehner AC *et al.* Chemical screening identifies filastatin, a small molecule inhibitor of *Candida albicans* adhesion, morphogenesis, and pathogenesis. *Proc Natl Acad Sci USA* 2013;**110**:13594–9.

Friedman ES, Bittinger K, Esipova TV *et al.* Microbes vs. chemistry in the origin of the anaerobic gut lumen. *Proc Natl Acad Sci USA* 2018;**115**:4170–5.

Gale CA, Bendel CM, McClellan M *et al.* Linkage of adhesion, filamentous growth, and virulence in *Candida albicans* to a single gene, *INT1*. *Science* 1998;**279**:1355–8.

Gerard R, Sendid B, Colombel JF *et al.* An immunological link between *Candida albicans* colonization and Crohn's disease. *Crit Rev Microbiol* 2015;**41**:135–9.

Ginos BNR, Navarro SL, Schwarz Y *et al.* Circulating bile acids in healthy adults respond differently to a dietary pattern characterized by whole grains, legumes and fruits and vegetables compared to a diet high in refined grains and added sugars: a randomized, controlled, crossover feeding study. *Metabolism* 2018;**83**:197–204.

Gu H, Zhang P, Zhu J *et al.* Globally optimized targeted mass spectrometry: reliable metabolomics analysis with broad coverage. 2015:12355-62.

Gu H, Carroll PA, Du J *et al.* Quantitative method to investigate the balance between metabolism and proteome biomass: starting from glycine. *Angew Chem Int Ed Engl* 2016;**55**:15646–50.

Guastalegname M, Russo A, Falcone M *et al.* Candidemia subsequent to severe infection due to *Clostridium difficile*: is there a link? *Clin Infect Dis* 2013;**57**:772–4.

Guinan J, Thangamani S. Antibiotic-induced alterations in taurocholic acid levels promote gastrointestinal colonization of *Candida albicans*. *FEMS Microbiol Lett* 2018;**365**:1-6.

Guinan J, Villa P, Thangamani S. Secondary bile acids inhibit *Candida albicans* growth and morphogenesis. *Pathog Dis* 2018;**76**:1-8.

Hager CL, Isham N, Schrom KP *et al.* Effects of a novel probiotic combination on pathogenic bacterial-fungal polymicrobial biofilms. *MBio* 2019;**10**:00338-19.

Hooper LV, Midtvedt T, Gordon JI. How host-microbial interactions shape the nutrient environment of the mammalian intestine. *Annu Rev Nutr* 2002;**22**:283–307.

Jasbi P, Wang D, Cheng SL *et al.* Breast cancer detection using targeted plasma metabolomics. *J Chromatogr B* 2019;**1105**:26–37.

Kantarcioglu AS, Kiraz N, Aydin A. Microbiota-Gut-brain axis: yeast species isolated from stool samples of children with suspected or diagnosed autism spectrum disorders and in vitro susceptibility against nystatin and fluconazole. *Mycopathologia* 2016;**181**:1–7.

Kelly CJ, Zheng L, Campbell EL *et al.* Crosstalk between microbiota-derived short-chain fatty acids and intestinal epithelial HIF augments tissue barrier function. *Cell Host Microbe* 2015;**17**:662–71.

Kennedy MJ, Volz PA. Ecology of *Candida albicans* gut colonization: inhibition of *Candida* adhesion, colonization, and dissemination from the gastrointestinal tract by bacterial antagonism. *Infect Immun* 1985;**49**:654–63.

Kennedy MJ, Volz PA, Edwards CA *et al.* Mechanisms of association of *Candida albicans* with intestinal mucosa. *J Med Microbiol* 1987;**24**:333–41.

Kim S, Covington A, Pamer EG. The intestinal microbiota: antibiotics, colonization resistance, and enteric pathogens. *Immunol Rev* 2017;**279**:90–105.

Kohli N, Crisp Z, Riordan R *et al.* The microbiota metabolite indole inhibits *Salmonella virulence*: involvement of the PhoPQ two-component system. *PLoS One* 2018;**13**:e0190613.

Krause R, Krejs GJ, Wenisch C *et al.* Elevated fecal *Candida* counts in patients with antibiotic-associated diarrhea: role of soluble fecal substances. *Clin Diagn Lab Immunol* 2003;**10**:167–8.

Krause R, Schwab E, Bachhiesl D *et al.* Role of *Candida* in antibiotic-associated diarrhea. *J Infect Dis* 2001;**184**:1065–9.

Langille MG, Zaneveld J, Caporaso JG *et al.* Predictive functional profiling of microbial communities using 16S rRNA marker gene sequences. *Nat Biotechnol* 2013;**31**:814–21.

Li CY, Dempsey JL, Wang D *et al.* PBDEs altered gut microbiome and bile acid homeostasis in male C57BL/6 Mice. *Drug Metab Dispos* 2018a;**46**:1226–40.

Li R, Grimm SA, Mav D *et al.* Transcriptome and DNA methylome analysis in a mouse model of diet-induced obesity predicts increased risk of colorectal cancer. *Cell Rep* 2018b;**22**:624–37.

Lo HJ, Kohler JR, DiDomenico B *et al.* Nonfilamentous *C. albicans* mutants are avirulent. *Cell* 1997;**90**:939–49.

Lustri BC, Sperandio V, Moreira CG. Bacterial chat: intestinal metabolites and signals in host-microbiota-pathogen interactions. *Infect Immun* 2017;**85**:00476-17.

Marteyn B, West NP, Browning DF *et al*. Modulation of *Shigella virulence* in response to available oxygen in vivo. *Nature* 2010;**465**:355–8.

Martin R, Albrecht-Eckardt D, Brunke S *et al*. A core filamentation response network in *Candida albicans* is restricted to eight genes. *PLoS One* 2013;**8**:e58613.

Mason KL, Erb Downward JR, Mason KD *et al*. *Candida albicans* and bacterial microbiota interactions in the cecum during recolonization following broad-spectrum antibiotic therapy. *Infect Immun* 2012;**80**:3371–80.

Meijer-Severs GJ, Joshi JH. The effect of new broad-spectrum antibiotics on faecal flora of cancer patients. *J Antimicrob Chemother* 1989;**24**:605–13.

Mendelsohn S, Pinsky M, Weissman Z *et al*. Regulation of the *Candida albicans* hypha-inducing transcription factor *Ume6* by the *CDK1* cyclins *Cln3* and *Hgc1*. *mSphere* 2017;**2**.

Miranda LN, van der Heijden IM, Costa SF *et al*. *Candida* colonisation as a source for candidaemia. *J Hosp Infect* 2009;**72**:9–16.

Mullineaux-Sanders C, Suez J, Elinav E *et al*. Sieving through gut models of colonization resistance. *Nat Microbiol* 2018;**3**:132–40.

Naseem S, Gunasekera A, Araya E *et al*. N-acetylglucosamine (GlcNAc) induction of hyphal morphogenesis and transcriptional responses in *Candida albicans* are not dependent on its metabolism. *J Biol Chem* 2011;**286**:28671–80.

Nerandzic MM, Mullane K, Miller MA *et al*. Reduced acquisition and overgrowth of vancomycin-resistant enterococci and *Candida* species in patients treated with fidaxomicin versus vancomycin for *Clostridium difficile* infection. *Clin Infect Dis* 2012;**55**:S121–6.

Neville BA, d'Enfert C, Bougnoux ME. *Candida albicans* commensalism in the gastrointestinal tract. *FEMS Yeast Res* 2015;**15**:1-15.

Nucci M, Anaissie E. Revisiting the source of candidemia: skin or gut? *Clin Infect Dis* 2001;**33**:1959–67.

O'Flaherty S, Briner Crawley A, Theriot CM *et al*. The lactobacillus bile salt hydrolase repertoire reveals niche-specific adaptation. *mSphere* 2018;**3**:00140-18.

Pande K, Chen C, Noble SM. Passage through the mammalian gut triggers a phenotypic switch that promotes *Candida albicans* commensalism. *Nat Genet* 2013;**45**:1088–91.

Piispanen AE, Hogan DA. PEPped up: induction of *Candida albicans* virulence by bacterial cell wall fragments. *Cell Host Microbe* 2008;**4**:1–2.

Ramirez-Perez O, Cruz-Ramon V, Chinchilla-Lopez P *et al*. The role of the gut microbiota in bile acid metabolism. *Ann Hepatol* 2017;**16**:s15–20.

Raponi G, Visconti V, Brunetti G *et al*. *Clostridium difficile* infection and *Candida* colonization of the gut: is there a correlation? *Clin Infect Dis* 2014;**59**:1648–9.

Reese AT, Cho EH, Klitzman B *et al*. Antibiotic-induced changes in the microbiota disrupt redox dynamics in the gut. *Elife* 2018;**7**:1-22.

Ridlon JM, Hylemon PB. Identification and characterization of two bile acid coenzyme A transferases from *Clostridium scindens*, a bile acid 7alpha-dehydroxylating intestinal bacterium. *J Lipid Res* 2012;**53**:66–76.

Ridlon JM, Kang DJ, Hylemon PB. Bile salt biotransformations by human intestinal bacteria. *J Lipid Res* 2006;**47**:241–59.

Ridlon JM, Kang DJ, Hylemon PB *et al*. Bile acids and the gut microbiome. *Curr Opin Gastroenterol* 2014;**30**:332–8.

Ridlon JM, Harris SC, Bhowmik S *et al*. Consequences of bile salt biotransformations by intestinal bacteria. *Gut Microbes* 2016;**7**:22–39.

Rizzatti G, Lopetuso LR, Gibiino G *et al*. Proteobacteria: a common factor in human diseases. *Biomed Res Int* 2017;**2017**:9351507.

Sahni V, Agarwal SK, Singh NP *et al*. Candidemia–an underrecognized nosocomial infection in Indian hospitals. *J Assoc Physicians India* 2005;**53**:607–11.

Samonis G, Gikas A, Anaissie EJ *et al*. Prospective evaluation of effects of broad-spectrum antibiotics on gastrointestinal yeast colonization of humans. *Antimicrob Agents Ch* 1993;**37**:51–3.

Schulte DM, Sethi A, Gangnon R *et al*. Risk factors for Candida colonization and Co-colonization with multi-drug resistant organisms at admission. *Antimicrob Resist Infect Control* 2015;**4**:46.

Seekatz AM, Theriot CM, Rao K *et al*. Restoration of short chain fatty acid and bile acid metabolism following fecal microbiota transplantation in patients with recurrent *Clostridium difficile* infection. *Anaerobe*. 2018;**53**:64-73.

Segata N, Izard J, Waldron L *et al*. Metagenomic biomarker discovery and explanation. *Genome Biol* 2011;**12**:R60.

Setiadi ER, Doedt T, Cottier F *et al*. Transcriptional response of *Candida albicans* to hypoxia: linkage of oxygen sensing and Efg1p-regulatory networks. *J Mol Biol* 2006;**361**:399–411.

Shi X, Wang S, Jasbi P *et al*. Database-assisted globally optimized targeted mass spectrometry (dgot-2019;ms): broad and reliable metabolomics analysis with enhanced identification. *Anal Chem* 2019;**91**:13737-45.

Shin NR, Whon TW, Bae JW. Proteobacteria: microbial signature of dysbiosis in gut microbiota. *Trends Biotechnol* 2015;**33**:496–503.

Shirtliff ME, Peters BM, Jabra-Rizk MA. Cross-kingdom interactions: *Candida albicans* and bacteria. *FEMS Microbiol Lett* 2009;**299**:1–8.

Sridharan GV, Choi K, Klemashevich C *et al*. Prediction and quantification of bioactive microbiota metabolites in the mouse gut. *Nat Commun* 2014;**5**:5492.

Stamatiades GA, Ioannou P, Petrikkos G *et al*. Fungal infections in patients with inflammatory bowel disease: a systematic review. *Mycoses* 2018;**61**:366–76.

Suez J, Elinav E. The path towards microbiome-based metabolite treatment. *Nat Microbiol* 2017;**2**:17075.

Synnott JM, Guida A, Mulhern-Haughey S *et al*. Regulation of the hypoxic response in Candida albicans. *Eukaryot Cell* 2010;**9**:1734–46.

Thangamani S, Guinan J, Wang S *et al*. Antibiotic-induced decreases in the levels of microbial-derived short-chain fatty acids promote gastrointestinal colonization of *Candida albicans*. *bioRxiv* 2018.

Theriot CM, Bowman AA, Young VB. Antibiotic-induced alterations of the gut microbiota alter secondary bile acid production and allow for *Clostridium difficile* spore germination and outgrowth in the large intestine. *mSphere* 2016;**1**:00045-15.

Theriot CM, Koumpouras CC, Carlson PE *et al*. Cefoperazone-treated mice as an experimental platform to assess differential virulence of *Clostridium difficile* strains. *Gut Microbes* 2011;**2**:326–34.

Theriot CM, Koenigsknecht MJ, Carlson PE, Jr. *et al*. Antibiotic-induced shifts in the mouse gut microbiome and metabolome increase susceptibility to *Clostridium difficile* infection. *Nat Commun* 2014;**5**:3114.

Toenjes KA, Munsee SM, Ibrahim AS *et al*. Small-molecule inhibitors of the budded-to-hyphal-form transition in the

pathogenic yeast *Candida albicans*. *Antimicrob Agents Ch* 2005;**49**:963–72.

Tso GHW, Reales-Calderon JA, Tan ASM *et al*. Experimental evolution of a fungal pathogen into a gut symbiont. *Science* 2018;**362**:589–95.

Vila T, Romo JA, Pierce CG *et al*. Targeting *Candida albicans* filamentation for antifungal drug development. *Virulence* 2017;**8**:150–8.

Vylkova S, Carman AJ, Danhof HA *et al*. The fungal pathogen *Candida albicans* autoinduces hyphal morphogenesis by raising extracellular pH. *MBio* 2011;**2**:e00055–11.

Wahlstrom A, Sayin SI, Marschall HU *et al*. Intestinal crosstalk between bile acids and microbiota and its impact on host metabolism. *Cell Metab* 2016;**24**:41–50.

Weingarden AR, Chen C, Bobr A *et al*. Microbiota transplantation restores normal fecal bile acid composition in recurrent *Clostridium difficile* infection. *Am J Physiol Gastrointest Liver Physiol* 2014;**306**:G310–9.

Wexler HM. Bacteroides: the good, the bad, and the nitty-gritty. *Clin Microbiol Rev* 2007;**20**:593–621.

Wiesner SM, Jechorek RP, Garni RM *et al*. Gastrointestinal colonization by *Candida albicans* mutant strains in antibiotic-treated mice. *Clin Diagn Lab Immunol* 2001;**8**:192–5.

Witchley JN, Penumetcha P, Abon NV *et al*. *Candida albicans* morphogenesis programs control the balance between gut commensalism and invasive infection. *Cell Host Microbe* 2019;**25**:432–443.e436.

Xu XL, Lee RT, Fang HM *et al*. Bacterial peptidoglycan triggers *Candida albicans* hyphal growth by directly activating the adenylyl cyclase Cyr1p. *Cell Host Microbe* 2008;**4**:28–39.

Yoon MY, Yoon SS. Disruption of the gut ecosystem by antibiotics. *Yonsei Med J* 2018;**59**:4–12.

Young VB, Schmidt TM. Antibiotic-associated diarrhea accompanied by large-scale alterations in the composition of the fecal microbiota. *J Clin Microbiol* 2004;**42**:1203–6.

Zhang Y, Klaassen CD. Effects of feeding bile acids and a bile acid sequestrant on hepatic bile acid composition in mice. *J Lipid Res* 2010;**51**:3230–42.

Zhu J, Djukovic D, Deng L *et al*. Colorectal cancer detection using targeted serum metabolic profiling. *J Proteome Res* 2014;**13**:4120–30.

Zuo T, Wong SH, Cheung CP *et al*. Gut fungal dysbiosis correlates with reduced efficacy of fecal microbiota transplantation in *Clostridium difficile* infection. *Nat Commun* 2018;**9**:3663.